Acoustic scattering from arbitrarily shaped three dimensional rigid bodies using method of moments solution with node based basis functions

B. Chandrasekhar[1]

Abstract: In this work, a novel numerical technique is presented to calculate the acoustic fields scattered by three dimensional rigid bodies of arbitrary shape using the method of moment's solution procedure. A new set of basis functions, namely, Node based basis functions are developed to represent the source distribution on the surface of rigid body and the same functions are used as testing functions as well. Both single layer formulation and double layer formulations are numerically solved using the same basis functions. The surface of the body is modeled by triangular patch modeling. Numerical technique presented in this paper, using these node based basis functions, is compared with the exact solutions wherever available and also with the edge based solutions [Chandrasekhar and Rao (2004)].

keyword: Acoustic Scattering, Method of Moments, Node based basis function, Boundary Integral Equations.

1 Introduction

In the recent past, there has been a growing demand for the development of faster, accurate and efficient algorithms to solve the acoustic scattering problem. This may be partly due to the developments in the digital computer technology and partly due to the ever increasing demand in the defense/commercial sectors. There are several formulations and algorithms to address the acoustic scattering problems based on T-matrix approach [Varadan and Varadan (1980), Varadan, Lakathia, and Varadan (1988), Tobocman (1984)], boundary integral equation method [Schuster and Smith (1985), Schuster (1985), Seybert, Soenarko, Rizzo, and Shippy (1985), Malbequi, Candel, and Rignot (1987)], and the method of moments solution [Harrington (1968), Rao and Raju (1989), Raju, Rao, and Sun (1991), Rao and Sridhara(1991) ,Rao, Raju, and Sun(1992), Sun and Rao (1992)].

All the formulations/algorithms have one common prob-

lem known as non uniqueness problem i.e. when the frequency of incident wave matches with the characteristic frequency of the surface S of the body, the solution breaks down. These characteristic frequencies happen to be resonance frequencies of the cavity formed by surface S of the body. There are two popular approaches which address this problem 1) Combined Helmholtz Integral Equation Formulation (CHIEF) [Schenck (1968)] 2) Burton and Miller's (BM) approach [Burton and Miller (1971)]. Although CHIEF is very popular, it is heuristic and prone to inaccuracies especially at higher frequencies. The BM approach is a mathematically proven method to eliminate non-uniqueness problem but it also suffers from a drawback, which is explained below.

BM procedure basically suggests developing and solving two separate formulations known as Single Layer Formulation (SLF) and Double Layer Formulation (DLF). Burton and Miller mathematically proved [Burton and Miller (1971)] that by combining the SLF and DLF with a complex constant, the internal resonance/non-uniqueness problem can be eliminated. Although SLF is relatively easier to solve, the DLF is much more difficult to solve numerically due to the presence of hyper-singular kernel in the integral equation. However, many researchers [Amini and Wilton (1986), Meyer, Bell, Zinn, and Stallybras (1978), Chien, Raliyah and Alturi (1990), Yan, Cui and Hung (2005)] attempted to implement the BM procedure to overcome the internal resonance problem. The usual procedure is to regularize the hyper–singular integral and the regularization technique is computationally very expensive and it is difficult to incorporate in a general-purpose code. Also, there are other methods which reduce the hyper singular kernel to a strongly singular kernel and their solution is based on based on Petrov-Galerkin schemes [Qian, Han, and Atluri (2004)] and collocation-based boundary element method [Qian, Han, Ufimtsev, and Atluri (2004)]. A de-singularized boundary integral formulation is also one of the recently proposed method [Callsen, von Estorff, and Zaleski (2004)] to overcome the problems of singularity.

[1] Supercomputer Education and Research Center, Indian Institute of Science, Bangalore - 560012, India.

Recently double layer formulation of BM approach was numerically solved by using method of moment's solution [Chandrasekhar and Rao (2004a)] and it is shown [Chandrasekhar and Rao (2004b)] that the internal resonance problem can be eliminated by combining SLF and DLF with a complex constant as suggested by Burton and Miller. Later, the same numerical solution procedure [Chandrasekhar and Rao (2005)] was extended to open bodies, intersecting bodies and other complex shaped closed bodies. This was achieved by selecting appropriate basis functions in the method of moment's solution and by simplifying the formulation with simple vector calculus. We also note that, the solution procedure mentioned in this paper, neither regularizes the hyper-singular integral nor implements complex integration schemes. The numerical procedure mentioned in the earlier work [Chandrasekhar and Rao (2004)] was based on the edge based basis functions and the size of the impedance matrix depends on the number of edges present in the triangular patch modeling. An attempt is made in this work, to reduce the size of the impedance matrix so that the computational time required for the solution of linear equations comes down.

In this work, a new set of basis functions, namely, Node based basis functions are developed to represent the source distribution and the same functions are used as testing functions as well. The surface of the closed body is modeled by triangular patch modeling and in this kind of modeling, the number of nodes are always less than the number of edges or faces. With this scheme, the size of the impedance matrix is very small compared to edge based solution [Chandrasekhar and Rao (2004)] or face based solution [Rao, Raju, and Sun (1992)] as the numerical solution is based on defining the basis functions on the nodes. As the storage matrix is smaller, time required for the solution of simultaneous linear system of equations is smaller and hence, much larger problems can be solved without increasing the solution time compared to the existing solutions based on method of moments [Rao, Raju, and Sun (1992), Chandrasekhar and Rao (2004a)].

2 Organization of a paper

In this paper, next section briefly describes the method of moment's solution procedure. Mathematical formulation is laid in section III for single layer and double layer formulations. In section IV, we describe the numerical solution procedure and derive matrix equations for SLF and DLF. Numerical results, based on the development of new basis function are given in sec V. Lastly we present some important conclusions drawn from this present work.

3 Outline of Method of Moments

Consider the deterministic equation

$$\mathbf{Lf} = \mathbf{g} \tag{1}$$

where $\mathbf{L}$ is a linear operator, $\mathbf{g}$ is a known function and $\mathbf{f}$ is an unknown function to be determined. Let $\mathbf{f}$ be represented by a set of known functions $\mathbf{f}_j$, $j = 1, 2, ..., N$ termed as basis functions in the domain of $\mathbf{L}$ as a linear combination, given by

$$\mathbf{f} = \sum_{n=1}^{N} \alpha_j \mathbf{f_j} \tag{2}$$

where α_j are scalar coefficients to be determined. Substituting Eq. 2 into Eq. 1, and using the linearity of L, we have

$$\sum_{n=1}^{N} \alpha_j \mathbf{Lf_j} = \mathbf{g} \tag{3}$$

where the equality is usually approximate. Let $(w_1, w_2, w_3, ...)$ define a set of testing functions in the range of $\mathbf{L}$. Now, taking the inner product of Eq. 3 with each w_i and using the linearity of inner product defined as $\langle \mathbf{f}, \mathbf{g} \rangle = \int_s \mathbf{f} \bullet \mathbf{g} \, ds$, we obtain a set of linear equations, given by

$$\sum_{n=1}^{N} \alpha_j \langle w_i, \mathbf{Lf_j} \rangle = \langle w_i, \mathbf{g} \rangle \quad i = 1, 2, ..., N \tag{4}$$

The set of equations in Eq. 4 may be written in the matrix form as

$$\mathbf{ZX} = \mathbf{Y} \tag{5}$$

which can be solved for $\mathbf{Z}$ using any standard linear equation solution methodologies. The simplicity, accuracy and efficiency of the method of moments lies in choosing proper set of basis/testing functions and applying to the problem at hand. In this work, we propose a special set of basis functions and a novel testing scheme to obtain accurate results using SLF and DLF.

4 Mathematical Formulation

Consider an acoustic wave with a pressure and velocity $(p^i, \mathbf{u}^i)$ incident on a three-dimensional arbitrarily shaped rigid body placed in a homogeneous medium of density ρ and speed of sound through the medium c. As the body is rigid, the acoustic wave gets scattered with a pressure and velocity $(p^s, \mathbf{u}^s)$. Here, we note that, incident fields are defined in the absence of the scattering body. The pressure and velocity fields of acoustic wave is related to the velocity potential Φ as $\mathbf{u} = -\nabla\Phi$ and $p = j\omega\rho\Phi$ assuming a harmonic time variation.

Using the potential theory and the free space Green's function, the scattered velocity potential is defined as

$$\Phi^s = \int_s \sigma\left(\mathbf{r}'\right) G\left(\mathbf{r}, \mathbf{r}'\right) ds' \tag{6}$$

for single layer formulation and

$$\Phi^s = \int_s \sigma\left(\mathbf{r}'\right) \frac{\partial G\left(\mathbf{r}, \mathbf{r}'\right)}{\partial n'} ds' \tag{7}$$

for double layer formulation.

Where $\mathbf{r}$ and $\mathbf{r}'$ are the position vectors of observation and source point, respectively, with respect to a global coordinate system O. Vectors $\mathbf{n}$ and $\mathbf{n}'$ are the unit normal vectors with respect to the observation point and source point respectively. σ is the source distribution over the surface of the body and $G\left(\mathbf{r}, \mathbf{r}'\right)$ is the free space Green's function, given by,

$$G\left(\mathbf{r}, \mathbf{r}'\right) = \frac{e^{-jk\mathbf{k}\bullet|\mathbf{r}-\mathbf{r}'|}}{4\pi|\mathbf{r}-\mathbf{r}'|} \tag{8}$$

For a rigid body, the normal derivative of total velocity potential, on the surface of the body vanishes. That is

$$\frac{\partial\left(\Phi^i + \Phi^s\right)}{\partial n} = 0 \tag{9}$$

$$\frac{\partial\Phi^s}{\partial n} = -\frac{\partial\Phi^i}{\partial n} \tag{10}$$

Substituting Eqs. 6 and 7. into Eq. 10,

$$\frac{\partial}{\partial n}\int_s \sigma\left(\mathbf{r}'\right) G\left(\mathbf{r}, \mathbf{r}'\right) ds' = -\frac{\partial\Phi^i}{\partial n} \tag{11}$$

for single layer formulation and

$$\frac{\partial}{\partial n}\int_s \sigma\left(\mathbf{r}'\right) \frac{\partial G\left(\mathbf{r}, \mathbf{r}'\right)}{\partial n'} ds' = -\frac{\partial\Phi^i}{\partial n} \tag{12}$$

For double layer formulation.

Eq. 11 can be re-written as

$$\frac{\sigma}{2} - \int_s \sigma\left(\mathbf{r}'\right) \frac{\partial G\left(\mathbf{r}, \mathbf{r}'\right)}{\partial n} ds' = -\frac{\partial\Phi^i}{\partial n} \tag{13}$$

The second term in the above equation is the integration over the surface excluding the principal value term i.e. $\mathbf{r} = \mathbf{r}'$. This integration can be evaluated using standard integration algorithms.

Following the procedures developed in [Maue (1949) and Mitzner (1966)], Eq. 12 may be written as

$$\int_s \mathbf{n} \bullet \mathbf{n}' k^2 \sigma(\mathbf{r}') G(\mathbf{r}, \mathbf{r}') \mathbf{ds}' + \int_s \left(\mathbf{n}' X \nabla'\sigma\right) \bullet \left(\mathbf{n} X \nabla G\right) ds' = \frac{\partial\Phi^i}{\partial n} \tag{14}$$

where $\mathbf{n}$ and $\mathbf{n}'$ are the unit normal vectors at $\mathbf{r}$ and $\mathbf{r}'$.

In the following sections, a novel numerical technique is developed using node based basis functions for both single layer and double layer formulations. Eq. 11 and Eq. 12 fail when the frequency of the incident field matches with the characteristic frequency of surface S. However, this internal resonance problem can be eliminated by combined layer formulation [Burton and Miller (1971)]. This paper focuses only on the numerical solution of the single layer and double layer formulations by developing a new set of basis functions called node based basis function.

5 Numerical Solution Procedure

Consider a three dimensional arbitrarily shaped body approximated by a triangular patches as shown in Fig. 1.

Let N_f, N_e and N_n represent the number of triangular patches, number of edges and number of nodes respectively on the surface of triangulated body. Consider a node n about which the basis function is defined in contrast to the basis functions defined with respect to edge as in [Chandrasekhar and Rao (2004)]. When the object is a closed one, all the nodes will have at least three triangular patches attached to it and at least three edges.

For illustration purposes, consider one such a node as shown in Fig. 2., where there are five triangular patches attached to it. Let $T_1, T_2, \ldots, T_5$ are the triangular patches
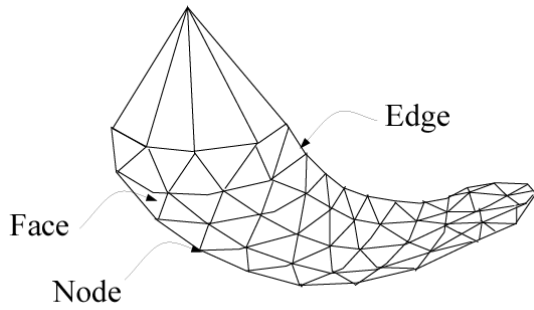
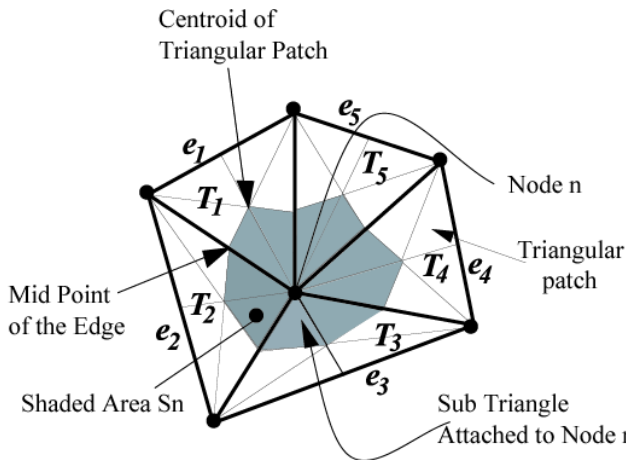**Figure 1** : Triangular patch modeling of an arbitrarily shaped three-dimensional body.

Figure 2 : Node based basis function and geometric parameters associated with the node.

and $e_1, e_2, \ldots, e_5$ are the edges connected to the node. The shaded region, shown in the Fig. 2. as S_n, is formed by joining the mid points of the edges to the centroids of adjacent triangular patches thus forming a closed boundary around the node.

Let there are p number of triangular patches attached to field node m and q number of triangular patches attached the source node n. By joining the node on which the basis function or weighting function is defined, to the centroid of the attached triangular patches, the shaded area on each triangular patch is divided into two sub triangles, resulting u number of sub triangles around field node m and v number of sub triangles around the source node n. In this paper, index x is used to represent the sub triangle attached to the field node and index y is used to

represent the sub triangle attached to the source node.

The node based basis function is defined over the shaded area as follows.

$$f_n = \begin{cases} 1 & \mathbf{r} \in S_n \\ 0 & Otherwise \end{cases} \tag{15}$$

The source distribution σ over the surface of the scattering object is approximated by

$$\sigma = \sum_{n=1}^{N_n} \alpha_n f_n \tag{16}$$

where α_n represent the unknown coefficients to be determined. The basis functions defined over the node has all advantages as edge based basis functions [see B. Chandrasekhar and S.M. Rao (2004)].

5.1 Derivation of matrix equations for Single Layer Formulation

We follow the Galarkin's approach by using the same basis functions defined in Eq. 15 as testing functions as well.

Testing Eq. 13 with a testing function

$$w_m \quad \left\langle w_m, \frac{\sigma}{2} \right\rangle - \left\langle w_m, \int_s \sigma(\mathbf{r}') \frac{\partial G(\mathbf{r},\mathbf{r}')}{\partial n} ds' \right\rangle = \left\langle w_m, -\frac{\partial \Phi^i}{\partial n} \right\rangle \tag{17}$$

Evaluating the first term of Eq. 17

$$\left\langle w_m, \frac{\sigma}{2} \right\rangle = \frac{1}{2} \int_s w_m \sigma(\mathbf{r}') \, ds = \frac{\sigma(\mathbf{r}')}{2} \sum_{x=1}^{u} A_m^x \tag{18}$$

where A_m^x is the area of sub triangle attached to the field node.

Evaluating the second term of Eq. 17

$$\left\langle w_m, \int_s \sigma(\mathbf{r}') \frac{\partial G(\mathbf{r},\mathbf{r}')}{\partial n} ds' \right\rangle = \int_s w_m \int_s \sigma(\mathbf{r}') \frac{\partial G(\mathbf{r},\mathbf{r}')}{\partial n} ds' \, ds = \sum_{x=1}^{u} A_m^{cx} \int_s \sigma(\mathbf{r}') \frac{\partial G(\mathbf{r_m^{cx}},\mathbf{r}')}{\partial n} ds' \tag{19}$$

Evaluating the right hand side of Eq. 17

$$\left\langle w_m, -\frac{\partial \Phi^i}{\partial n} \right\rangle = -\int_s w_m \frac{\partial \Phi^i}{\partial n} ds = -\sum_{x=1}^{u} A_m^{cx} \frac{\partial \Phi^i}{\partial n} \tag{20}$$

Substituting the source expansion defined in Eq. 16 into Eq. 18 and Eq. 19, results in a system of linear equations of size $N_n X N_n$, which can be represented in the matrix form as

$$\mathbf{Z}_{slf}\mathbf{X} = \mathbf{Y} \tag{21}$$

where $\mathbf{Z}_{slf}$ is the impedance matrix of the single layer formulation of size $N_n X N_n$, $\mathbf{X}$ and $\mathbf{Y}$ are the column vectors of size N_n. The elements of $\mathbf{Z}_{slf}, \mathbf{X}$ and $\mathbf{Y}$ are given below.

$$\mathbf{Z}_{slf}^{mn} = \begin{cases} \frac{1}{2}\sum\limits_{x=1}^{u} A_m^x & for\, m = n\, and\, x = y \\ \\ -\sum\limits_{x=1}^{u}\sum\limits_{y=1}^{v} A_m^x \int_s \frac{\partial G\left(\mathbf{r}_m^{cx},\mathbf{r}_n^{cy}\right)}{\partial n_m^c} ds' & otherwise \end{cases} \tag{22}$$

and

$$\mathbf{Y}^m = -\sum\limits_{x=1}^{u} A_m^x \frac{\partial \Phi^i}{\partial n_m^x} \tag{23}$$

Once the elements of the impedance matrix $\mathbf{Z}$ and the forcing vector $\mathbf{Y}$ are determined, one may solve the linear system of equations, Eq. 21, for the unknown vector $\mathbf{X}$.

5.2 *Derivation of matrix equations for Double Layer Formulation*

Testing Eq. 14 with the functions defined in Eq. 15,

$$\begin{aligned} &\langle w_m, \int_s \mathbf{n} \bullet \mathbf{n}' k^2 \sigma(r') G(\mathbf{r},\mathbf{r}') ds' \rangle \\ &+ \langle w_m, \int_s (\mathbf{n}' x \nabla' \sigma) \bullet (\mathbf{n} X \nabla G)\, ds' \rangle \\ &= \left\langle w_m, \frac{\partial \Phi^i}{\partial n} \right\rangle \end{aligned} \tag{24}$$

Taking the first term for evaluation,

$$\begin{aligned} &\langle w_m, \int_s \mathbf{n} \bullet \mathbf{n}' k^2 \sigma(\mathbf{r}') G(\mathbf{r},\mathbf{r}') ds' \rangle \\ &= \int_s w_m \int_s \mathbf{n} \bullet \mathbf{n}' k^2 \sigma(\mathbf{r}') G(\mathbf{r},\mathbf{r}') ds' ds \\ &= \sum\limits_{x=1}^{u} A_m^x \mathbf{n}_m^x \bullet \int_s \mathbf{n}' k^2 \sigma(\mathbf{r}') G(\mathbf{r},\mathbf{r}') ds' \end{aligned} \tag{25}$$

where $\mathbf{n}_m^x$ represent the unit normal vectors of the sub triangle connected to the $\mathbf{m}^{th}$ node. We also note that the double surface integration in Eq. 25 is converted to a single surface integral by approximating the integrand at the centroid of the sub triangle attached to $\mathbf{m}^{th}$ node and multiplying by the area of the sub triangle as before.

To evaluate the second term in the Eq. 24, we follow the similar procedure mentioned in [Chandrasekhar and
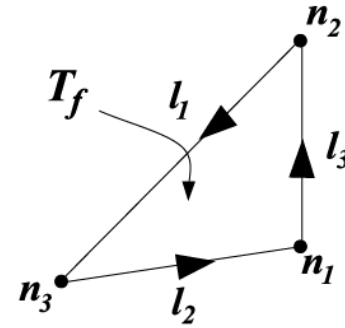

Figure 3 : triangular patch T_f and associated edges and nodes.

Rao (2004)], but node based basis function are used in contrast to the edge based basis functions. The advantages of using the node based basis function are already mentioned in the earlier section.

Let us define, $\mathbf{J}' = \mathbf{n}' X \nabla' \sigma$ and the vector $\mathbf{J}'$ is again approximated by a new set of basis function. We have,

$$\mathbf{J}' = \sum\limits_{f=1}^{N_f} \mathbf{g}_f(\mathbf{r}') \tag{26}$$

where $\mathbf{g}_f$ is spread over the triangular patch and assumed to be constant. Since $\mathbf{g}_f$ is not an independent quantity, a relationship between α_n, f_n and $\mathbf{g}_f$ may be derived as follows:

Consider the triangular patch T_f with associated non-boundary edges $\mathbf{l}_1, \mathbf{l}_2, \mathbf{l}_3$ and nodes $\mathbf{n}_1, \mathbf{n}_2, \mathbf{n}_3$ as shown in the Fig. 3.

Then, using well-known Stoke's theorem and simple vector calculus, $\mathbf{J}' = \mathbf{n}' X \nabla' \sigma$ may be re-written as

$$\begin{aligned} \int_s \mathbf{J}' ds' &= \int_s \mathbf{n}' X \nabla' \sigma\, ds' \\ &= \oint_{C_e} \sigma' \mathbf{dl}' \\ &= \frac{\alpha_1 f_1 \mathbf{l}_1 + \alpha_2 f_2 \mathbf{l}_2 + \alpha_3 f_3 \mathbf{l}_3}{2} \end{aligned} \tag{27}$$

where C_e is the contour bounding the triangle T_f and $\mathbf{l}_i$, $i = 1, 2, 3$ represent the edge vectors as shown in the Fig. 3. Noting that,

$$\begin{aligned} \int_s \mathbf{J}' ds' &= \int_s \mathbf{g}_f ds' \\ &= \mathbf{g}_f A_f \end{aligned} \tag{28}$$

where A_f is the area of the triangular patch attached to the source node.

$$\mathbf{g}_f = \frac{1}{A_f} \int_s \mathbf{J}' ds' \qquad (29)$$

substituting Eq. 27 in Eq. 29, we get

$$\mathbf{g}_f = \frac{1}{2A_f} (\alpha_1 f_1 \mathbf{l}_1 + \alpha_2 f_2 \mathbf{l}_2 + \alpha_3 f_3 \mathbf{l}_3) \qquad (30)$$

This is the required relationship between $\mathbf{g}_f$ and f_n.

Taking the testing operation on the second term of Eq. 24 and following the procedure mentioned in [Chandrasekhar and Rao (2004)], but with the node based basis functions,

$$\langle w_m, \int_s \mathbf{J}' \bullet (\mathbf{n} X \nabla G) \, ds' \rangle = \oint_{Cm} \mathbf{A} \bullet \mathbf{dl}$$
$$= \frac{\mathbf{l}_m}{2} \bullet \left(\sum_{x=1}^{p} \mathbf{A} \left(\mathbf{r}_m^{cfx} \right) \right) \qquad (31)$$

where $\mathbf{A} = \int_s \mathbf{J}' G ds'$, p is the number of triangular patches attached to the field node and $\mathbf{r}_m^{cfx}$ is the position vector for the centroid of triangular patch attached to the field node. The expression for the testing operation on right hand side of the Eq. 24 is as same as that of single layer formulation, i.e. Eq. 23

Substituting Eq. 23, Eq. 25 and Eq. 31 in Eq. 24, we get

$$\sum_{x=1}^{u} A_m^x \mathbf{n}_m^x \bullet \int_s n' k^2 \sigma(\mathbf{r}') G(\mathbf{r}_m^{cx}, \mathbf{r}') ds'$$
$$+ \frac{\mathbf{l}_m}{2} \bullet \left(\sum_{x=1}^{p} \mathbf{A} \left(\mathbf{r}_m^{cfx} \right) \right) = \sum_{x=1}^{u} A_m^x \frac{\partial \Phi^i}{\partial n_m^x} \qquad (32)$$

Substituting the source expansion defined in Eq. 16 and Eq. 15, it results into a system of linear equations which can be expressed in matrix form as

$$\mathbf{Z}_{dlf} \mathbf{X} = \mathbf{Y} \qquad (33)$$

where $\mathbf{Z}_{dlf}$ is the impedance matrix for double layer formulation of size $N_n X N_n$, $\mathbf{X}$ and $\mathbf{Y}$ are column vector of size N_n.

$$\mathbf{Z}_{dlf}^{mn} = \sum_{x=1}^{u} \sum_{y=1}^{v} A_m^x \mathbf{n}_m^x \bullet \mathbf{n}_n^y \int_s k^2 \sigma(\mathbf{r}_n^{cy}) G(\mathbf{r}_m^{cx}, \mathbf{r}_n^{cy}) ds'$$
$$+ \frac{\mathbf{l}_m}{2} \bullet \frac{\mathbf{l}_n}{2A_{fn}} \left(\sum_{x=1}^{p} \sum_{y=1}^{q} \int_{sf} G \left(\mathbf{r}_m^{cfp}, \mathbf{r}_n^{cfq} \right) ds' \right) \qquad (34)$$

Note that the integration on the first term of right hand side of the above equation is on the sub triangle attached to the source node and the integration on the second term is on the triangular patch attached to the source node.

$$\mathbf{Y}^m = \sum_{x=1}^{u} A_m^x \frac{\partial \Phi^i (\mathbf{r}_m^{cx})}{\partial n_m^x} \qquad (35)$$

where

A_m^x = Area of the sub triangle attached to the field node.

A_{fn} = Area of the triangular patch attached to the source node.

$\mathbf{r}_m^{cx}$ = Position vector for the centroid of the xth sub triangle attached to field node.

$\mathbf{r}_n^{cy}$ = Position vector for the centroid of the yth sub triangle attached to source node.

$\mathbf{r}_m^{cfp}$ = Position vector for the centroid of the pth triangular patch attached to field node.

$\mathbf{r}_n^{cfq}$ = Position vector for the centroid of the qth triangular patch attached to source node.

Integrals appearing in Eq. 22 and Eq. 34 may be evaluated using the techniques mentioned in [Wilton, Rao, Glisson, Schaubert, Al-Bundak, and Bulter (1984) and Hammer, Marlowe, and Stroud (1956)] for an accurate solution, as the former contains singular kernels.

For a plane wave incidence, we set

$$\Phi^i = e^{jk\mathbf{k} \bullet \mathbf{r}} \qquad (36)$$

where the propagation vector $\mathbf{k}$ is

$$\mathbf{k} = \sin\theta_0 \cos\phi_0 \mathbf{n}_x + \sin\theta_0 \sin\phi_0 \mathbf{n}_y + \cos\theta_0 \mathbf{n}_z \qquad (37)$$

and (θ_0, ϕ_0) defines the angles of arrival of the plan wave in the conventional spherical co-ordinate system.

Once the elements of the impedance matrix $\mathbf{Z}$ and the forcing vector $\mathbf{Y}$ are determined, one may solve the linear system of equations, Eqs. 21 and 33, for the unknown vector $\mathbf{X}$.

6 Numerical Results

In this section, the numerical solution developed in the above section is validated against exact solution wherever available and against the edge based solution wherever exact solutions are not available. The geometries
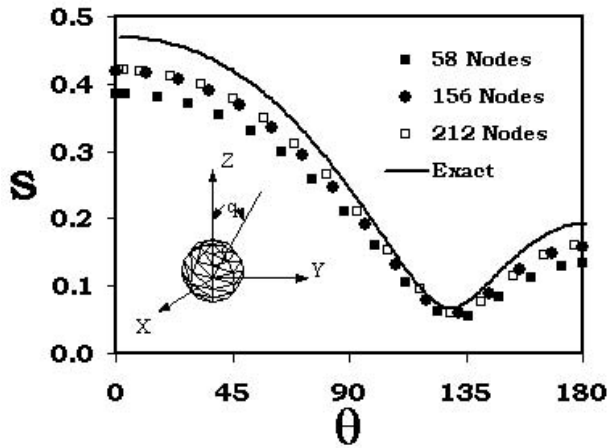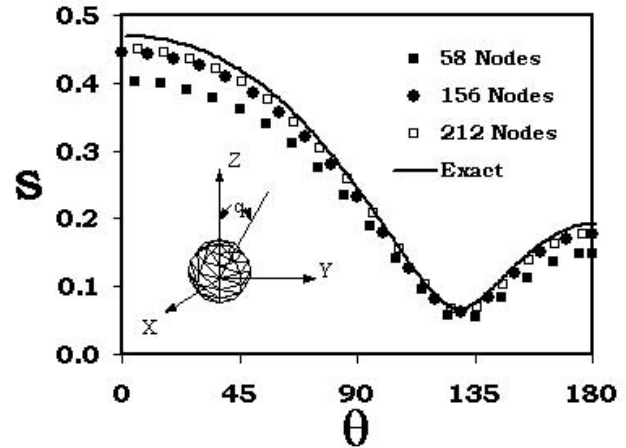
Figure 4 : Scattering cross section versus polar angle for an acoustically rigid sphere of radius 1m, subjected to an axially incident plane wave of $k = 1\,rad/m$, based on Single layer formulation (SLF).

Figure 5 : Scattering cross section versus polar angle for an acoustically rigid sphere of radius 1m, subjected to an axially incident plane wave of $k = 1\,rad/m$, based on Double layer formulation (DLF).

considered here are simple canonical shapes like Sphere, Cube, Cylinder and a Cone. For all these cases, the body is placed at the center of the co-ordinate system and a plane wave with $k = 1\,rad/m$, traveling along –Z axis is incident on the body. Here, We note that, no convergence study is carried out to ascertain the optimum number of nodes required to obtain certain degree of accuracy. The scattering cross section is defined by

$$
\begin{aligned}
S &= 4\pi \left| \frac{\Phi^s}{\Phi^i} \right|^2 \\
&\approx \frac{1}{4\pi} \left| \sum_{n=1}^{N_n} \alpha_n \left[\sum_{y=1}^{v} A_n^y \mathbf{n}_n^y \bullet \mathbf{r}_n^y e^{jk n_{\mathbf{n}}^y \bullet \mathbf{r}_n^y} \right] \right|^2
\end{aligned} \tag{38}
$$

As a first case, a sphere of radius $1m$ is considered with a triangular patch modeling. The modeling is done by dividing the θ and ϕ direction into eight equal segments each and the complete modeling procedure is described in [Chandrasekhar and Rao (2004)]. This results into 58 nodes, 112 faces and 168 edges on the surface of the sphere. Fig. 4. shows the scattering cross section as a function of polar angle Θ for the rigid sphere based on the SLF.

It is evident from the figure that, the method of moments solution based on the node based basis functions matches well with the exact solution [Bowman, Senior and Uslenghi (1969)]. The discrepancy between the two solutions can be attributed to insufficient number of unknowns and the fact that the surface area of the triangu-

lated sphere is less than that of the actual sphere.

In order to demonstrate the convergence of the solution, sphere is modeled with 156 nodes, 308 faces and 462 edges as well as with 212 nodes, 420 faces and 630 edges. The scattering cross section of these two cases is also shown in the Fig. 4. For all the above cases the DLF solution is also given in the Fig. 5. which also very well matches with the exact solution. Next, Fig. 6. shows the comparison between Node based solution with the edge based solution as this type of comparison is used for the cases where exact solutions are not available. Fig. 7. and Fig. 8. show the scattering cross section as function of polar angle for the case of rigid sphere with a radius of 2m for SLF and DLF respectively. The solution for SLF case can be further improved by increasing the number of unknowns. However, the DLF solution well matches with the exact solution even for $ka = 2$.

Next, we consider the case of a cube with side length $l = 1m$. The case of a cube presents a challenging task of handling sharp edges and corners. To obtain a triangular patch model, each side of the cube is divided into 4 equal segments resulting in 96 square patches and 98 nodes on the cube. By joining the diagonals, we get 192 triangular patches and 288 edges. Fig. 9. shows the scattering cross section S as a function of Θ. It is evident from the figure that the constant basis functions defined over an node for SLF and DLF compare very well with that of edge based SLF and DLF. Also, note that even though the
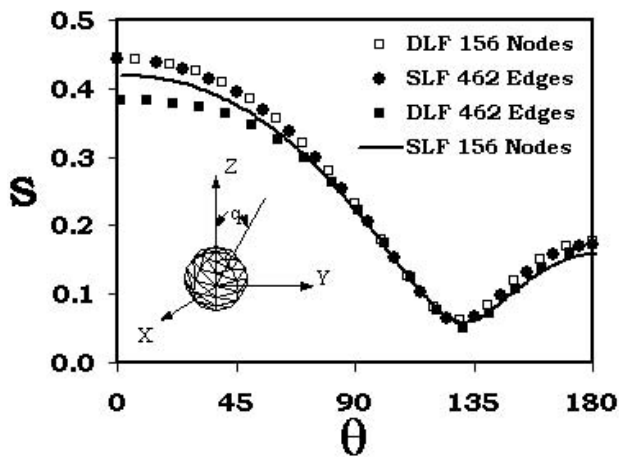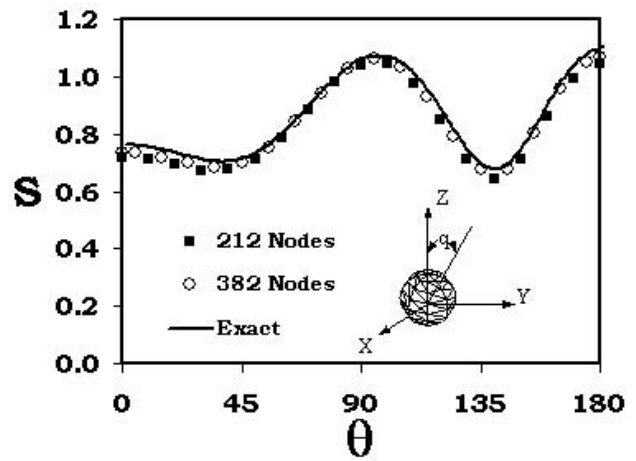
Figure 6 : Scattering cross section versus polar angle for an acoustically rigid sphere of radius 1m, subjected to an axially incident plane wave of $k = 1\,rad/m$, based on SLF and DLF.
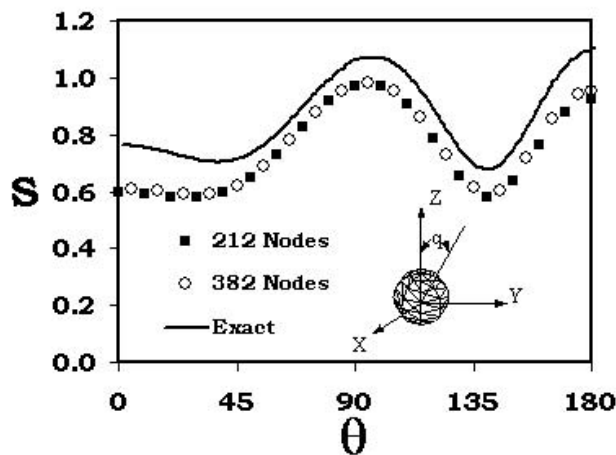

Figure 8 : Scattering cross section versus polar angle for an acoustically rigid sphere of radius 2m, subjected to an axially incident plane wave of $k = 1\,rad/m$, based on Double layer formulation (DLF).

Figure 7 : Scattering cross section versus polar angle for an acoustically rigid sphere of radius 2m, subjected to an axially incident plane wave of $k = 1\,rad/m$, based on Single layer formulation (SLF).
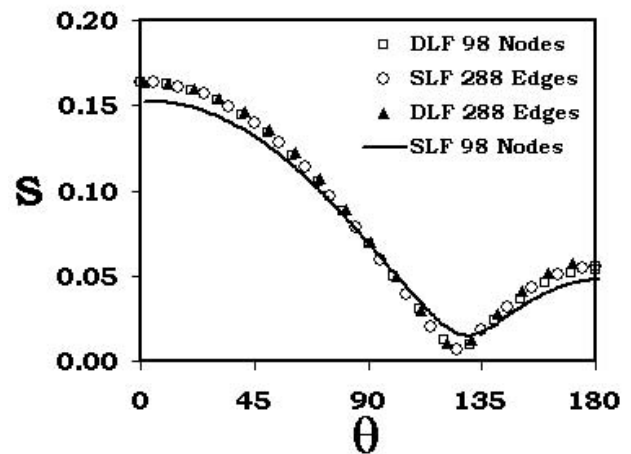

Figure 9 : Scattering cross section versus polar angle for an acoustically rigid cube of length 1m, subjected to an axially incident plane wave of $k = 1\,rad/m$, based on SLF and DLF.

basis functions are defined on sharp edges and corners, the numerical results are fairly

accurate. Finally, we note that the node-based conventional boundary integral methods [Schuster and Smith (1985),Schuster (1985), Seybert, Soenarko, Rizzo, and Shippy (1985), Malbequi, Candel, Rignot (1987)] need complex calculations to obtain accurate results for this geometry.

As a third example, we consider the case of a finite cylinder of height 2.0m and 1.0m radius. The triangular patch modeling of the cylinder is obtained by dividing the length and circumference into 8 and 10 uniform segments, respectively, resulting in 80 rectangular patches. By joining the diagonals, we obtain 160 triangular patches. The cylinder is closed on both ends by circular disks which are modeled by and additional 70 triangular patches each. Thus, in total we have 300 patches
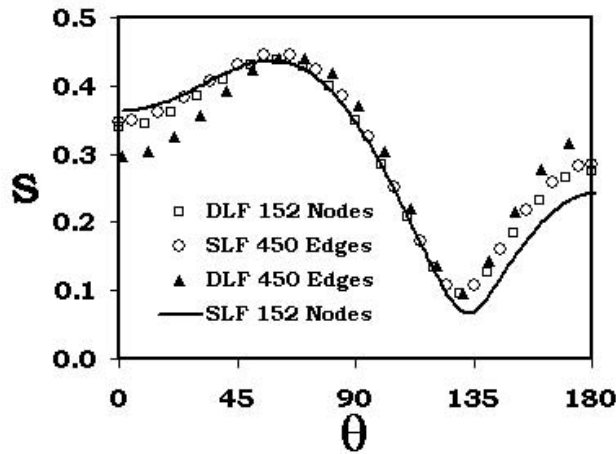
Figure 10 : Scattering cross section versus polar angle for an acoustically rigid cylinder of radius 1m and height 2m, subjected to an axially incident plane wave $k = 1\,rad/m$, based on SLF and DLF.

Figure 11 : Scattering cross section versus polar angle for an acoustically rigid cone of radius 1m and height 1m, subjected to an axially incident plane wave $k = 1\,rad/m$, based on SLF and DLF.

and 450 edges for this geometry. Fig. 10. shows the scattering cross section S as a function of Θ. For this case also, we note good comparison for SLF and DLF results.

Lastly, we consider a cone of 1m height and 1m radius. The cone has a sharp corner at the tip which is difficult to handle using node-based BIE methods. Using a similar discretization scheme as in the case of finite cylinder, the cone is divided into 220 patches resulting in 330 edges. Fig. 11. shows the scattering cross section S as a function of Θ which compares very well with the SLF result.

7 Conclusions

In this work, we presented a novel numerical technique implementing the method of moment's solution. Node based basis functions are defined to reduce the size of impedance matrix and hence the time required for solving the linear system of equations. Triangular patch modeling is used to approximate the surface of the scattering body. The scattering problem is formulated using SLF and DLF. SLF and DLF are numerically solved using same basis functions. The numerical results of the SLF and DLF based on the node based basis functions are compared with exact solutions wherever available, and edge based basis functions for various geometries
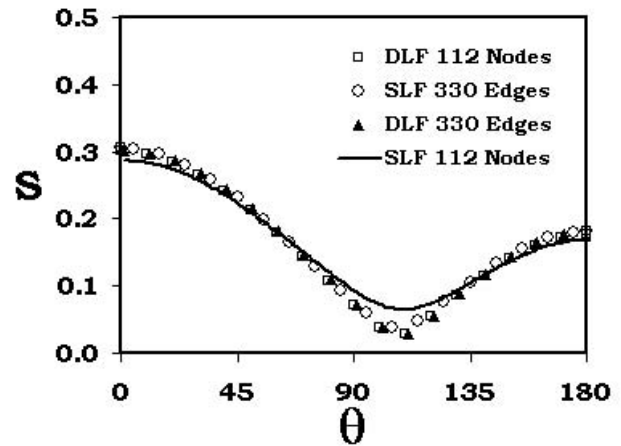
of canonical shapes. However, no comparison is made in this paper on the accuracy of node based versus edge based schemes. It is clearly evident from the numerical results that, schemes based on node based basis functions converge towards the exact solutions with higher number of nodes and have advantage over the edge based basis functions from the computational complexity perspective.

Although the numerical solution procedure presented, results in a smaller impedance matrix compared to the edge based solution, the computational time required for filling the impedance matrix in the Node based basis functions case is slightly higher than that of Edge based basis functions. However, comparing the computational complexity of solution of simultaneous equations, node based basis functions has an advantage over the edge based basis functions and the excess computational time required for filling the matrix is relatively negligible.

Further research is under progress to extend the node based basis functions to solve the internal resonance problem by implementing the combined layer formulation, acoustic scattering from open, intersecting and fluid bodies.

References

Amini, S.; Wilton, D.T. (1986): An investigation of Boundary element methods for the exterior acoustic

problem. *Computational Methods in Applied Mechanical Engineering*, vol 54, pp. 49-65.

Bowman, J.J.; Senior, T.B.A.; Uslenghi, P.L.E. (1969): Electromagnetic and Acustic Scattering by Simple Shapes North-holland, Amsterdam.

Burton, A.J.; Miller, G.F. (1971): The application of integral equation methods to the numerical solution of some exterior boundary value problems. *Proceedings of Royal Society, London* vol A323, pp. 601-618 .

Callsen, S.; von Estorff, O.; Zaleski, O. (2004): Direct and Indirect Approach of a Desingularized Boundary Element Formulation for Acoustical Problems. *CMES: Computer Modeling in Engineering & Sciences*, CMES, Vol. 6, No. 5, pp. 421-430

Chandrasekhar, B.; Rao, S.M. (2004a): Acoustic scattering from rigid bodies of arbitrary shape –double layer formulation. *Journal of Acoustical Society of America,* vol 115, pp. 1926-1933.

Chandrasekhar, B.; Rao, S.M. (2004b): Elimination of internal resonance problem associated with acoustic scattering by three-dimensional rigid body, *Journal of Acoustical Society of America,* vol 115, pp. 2731-2737.

Chandrasekhar, B.; Rao, S.M. (2005): Acoustic Scattering from Complex Shaped Three Dimensional Structures, *CMES: Computer Modeling in Engineering & Sciences*, Vol. 8, No. 2, pp. 105-118.

Chien, C.C.; Raliyah, H.; Alturi, S.N. (1990): An effective method for solving the hyper singular integral equations in 3-D acoustics. *Journal of Acoustical Society of America*, vol 88, pp. 918-937.

Hammer, P.C.; Marlowe, O.P.; Stroud, A.H. (1956): Numerical integration over simplxes and cones, *Math. Tables Aids Comp.* vol 10, pp. 130-138.

Harrington, R.F. (1968): Field computation by Method of Moments. *MacMillan, New York.*

Malbequi, P.; Candel, S.M. ; Rignot, E. (1987):, Boundary integral calculations of scattered fields : Application of spacecraft launcher. *Journal of Acoustical Society of America.* vol 82, pp. 1771-1781.

Maue, A.W. (1949):Zur Formulierung eines allgemeinen Beugungsproblems durch eine Integralgleichung. *Journal of Physics*, vol 126, pp. 601-618

Meyer, W. L.; Bell, W.A.; Zinn, B.T.; Stallybras, M. P. (1978): Boundary integral solutions of three dimensional acoustic radiation problems. *Journal of Sound and Vibration*, vol 59, pp. 245-262.

Mitzner, K.M. (1966): Acoustic scattering from an interface between media of greatly different density. *Journal of Mathematical Physics.* vol 7, pp. 2053-2060.

Qian, Z.Y.; Han, Z.D.; Atluri, S.N. (2004): Directly Derived Non-Hyper-Singular Boundary Integral Equations for Acoustic Problems, and Their Solution through Petrov-Galerkin Schemes, *CMES: Computer Modeling in Engineering & Sciences*, CMES, Vol. 5, No. 6, pp. 541-562

Qian, Z.Y.; Han, Z.D.; Ufimtsev, P.; Atluri, S.N. (2004): Non-Hyper-Singular Boundary Integral Equations for Acoustic Problems, Implemented by the Collocation-Based Boundary Element Method, *CMES: Computer Modeling in Engineering & Sciences*, CMES, Vol. 6, No. 2, pp. 133-144.

Raju, P.K.; Rao, S. M.; Sun, S.P. (1991): Application of the method of moments to acoustic scattering from multiple infinitely long fluid filled cylinders. *Computers and Structures.* vol 39}, pp. 129-134.

Rao, S.M.; Raju, P.K. (1989): Application of Method of moments to acoustic scattering from multiple bodies of arbitrary shape. *Journal of Acoustical Society of America.* vol 86, pp. 1143-1148.

Rao, S.M.; Sridhara, B.S. (1991): Application of the method of moments to acoustic scattering from arbitrary shaped rigid bodies coated with lossless, shearless materials of arbitrary thickness. *Journal of Acoustical Society of America.* vol 90, pp. 1601-1607.

Rao, S. M.; Raju, P.K.; Sun, S.P. (1992): Application of the method of moments to acoustic scattering from fluid-filled bodies of arbitrary shape. *Communications in Applied Numerical Methods*, vol 8}, pp. 117-128.

Schenck, H.A (1968): Improved integral formulation for acoustic radiation problems. *Journal of Acoustical Society of America.* vol 44, pp. 41-58.

Schuster, G.T.; Smith, L.C. (1985): A comparison and four direct boundary integral methods. *Journal of Acoustical Society of America.* vol 77, pp. 850-864.

Schuster, G.T. (1985): A hybrid BIE + Born series modeling scheme: Generalized Born series. *Journal of Acoustical Society of America.* vol 77, pp. 865-879.

Seybert, A.F.; Soenarko, B. ; Rizzo, F.J.; Shippy, D.J. (1985): An advanced computation method for radiation and scattering acoustic waves in three dimensions. *Jour-*

nal of Acoustical Society of America. vol 77, pp. 362-368.

Sun, S.P.; Rao, S. M. (1992): Application of the method of moments to acoustic scattering from multiple infinitely long fluid-filled cylinders using three different formulation. *Computers and Structures.* vol 43, pp. 1147-1153.

Tobocman, W. (1984): Calculation of acoustic wave scattering by means of the Helmholtz integral equation I. *Journal of Acoustical Society of America.* vol 76, pp. 599-607.

Tobocman, W. (1984): Calculation of acoustic wave scattering by means of the Helmholtz integral equation II. *Journal of Acoustical Society of America.* vol 76, pp. 1549-1554.

Varadan, V.K.; Lakathia, A.; Varadan, V.V (1988):, Comments on recent criticism of the T-Matrix method. *Journal of Acoustical Society of America.* vol 84, pp. 2280-2284.

Varadan, V.K.; Varadan, V.V (1980): Acoustic, Electromagnetic and Elastic wave scattering- Focus on the T-Matrix approach. *Pergamon, NewYork.*

Wilton, D.R.; Rao, S.M.; Glisson, A.W.; Schaubert, D.H.; Al-Bundak, O.M.; Bulter, C.M. (1984): Potential Integrals for uniform and linear source distributions on polygons and polyhedra domains. *IEEE transactions, Antennas Propagation.* vol AP-32, pp. 276-281.

Yan, Z.Y.; Cui, F. S.; Hung, K. C. (2005): Investigation on the Normal Derivative Equation of Helmholtz Integral Equation in Acoustics. *CMES: Computer Modeling in Engineering & Sciences*, Vol. 7, No. 1, pp. 97-106.